Human cortical areas are sparsely connected: Combining histology with diffusion MRI to estimate the absolute number of axons

Burke Q. Rosen[1*], Eric Halgren[1,2]

[1]Neurosciences Graduate Program, University of California, San Diego, La Jolla CA 92093
[2]Depts. of Neurosciences & Radiology, University of California, San Diego, La Jolla CA 92093

[*]bqrosen@health.ucsd.edu
3510 Dunhill St.
San Diego, CA 92101
858-405-9660

Author Roles:
E.H. : conceptualization, supervision, funding acquisition, writing – original draft preparation, writing review & editing
B.Q.R. : investigation, formal analysis, data curation, methodology, software, visualization, writing – original draft preparation, writing review & editing

Competing Interest Statement:
The authors declare no competing interests.

Keywords:
diffusion MRI | structural connectivity | white matter | neuroanatomy | Human Connectome Project

Abstract The tracts between cortical areas are conceived as playing a central role in cortical information processing, but their actual numbers have never been determined. Here we estimate the absolute number of axons linking cortical areas from a whole-cortex diffusion-MRI (dMRI) connectome, calibrated using the histologically-measured callosal fiber density. Median connectivity is estimated as ~2,700 axons between cortical areas within-hemisphere and ~540 axons interhemispherically, with axons connecting functionally-related areas surprisingly sparse. These results challenge models that require direct transmission of detailed information between cortical areas, rather suggesting that cortical integration mainly relies on the extremely dense local connections.

Introduction

The major tracts connecting cortical areas have long been central to models of information-processing in the human brain [1]. Such models have been refined and applied to development and disease with the advent of diffusion-MRI or dMRI, [2]. However, dMRI only provides *relative* connectivity, not the absolute number of axons. Relative connectivity is very useful in many circumstances but more constraints would be possible if the absolute number of axons connecting different cortical areas could be estimated. We find that routinely observed widespread functional synchronization belies a surprising small absolute number of long range axons connecting functionally-related areas.

Materials and Methods

The basic principle of our method is very simple. Given a dMRI-based measure of total interhemispheric connectivity in arbitrary units and the physical number of axons traversing the corpus callosum, the conversion factor between the two can be obtained by dividing the first by the second. Specifically, we started with the total interhemispheric tractography strength reported in our dMRI connectome of the Human Connectome Project (HCP) cohort [3]. For each individual, the cross-sectional area of the corpus callosum was obtained using the standard FreeSurfer structural MRI pipeline [4]. Multiplying this number by a histologically ascertained callosal fiber density [5] yields an estimate of the number of axons traversing an individual's corpus callosum. Dividing this count by individuals' interhemispheric dMRI streamline value yields the conversion ratio from the arbitrarily-

77 scaled dMRI metric to the absolute number of axons. Note that this procedure does not at all depend
78 on the scale of the dMRI metric, requiring only that it be proportional to absolute number of fibers.
79 This proportionality has been observed in a comparison of dMRI and retrograde tracing in macaques
80 [6]. Therefore, while the ratio itself is study-specific, the procedure can be applied to any dMRI
81 tractography method or parameter set. It only requires that the dMRI method return a continuous
82 distribution of connectivity values and have reasonably similar sensitivity to callosal and ipsilateral fiber
83 tracts. For detailed methodology, see S1 Appendix: Extended Methods.

84 **Results**

85 Our previous dMRI study [3] includes estimated tractography streamlines among all 360 parcels of the
86 HCP-MMP1.0 atlas [7] for each of the 1,065 individuals in the HCP dMRI cohort. The sum connectivity
87 between the 180 left hemisphere cortical parcels and the 180 right (180^2 parcel pairs) constitutes the
88 total callosal connectivity, on average 1.25×10^8 streamlines. Comparing linear regressions of distance-
89 matched log-transformed streamlines, we found no difference between the slope or intercept of inter-
90 and intrahemispheric connections; within the common distance domain a paired r-test showed no
91 difference in correlation, $p = 0.58$. Based on our assumed fiber density of 1.6×10^5 axons/mm^2 [5] and
92 measured callosal cross-sectional area (mean = 689.45mm^2), we estimate this cohort to have 1.1×10^8
93 callosal fibers on average. The mean quotient between these two quantities is 0.87 axons-per-
94 streamline, a ratio specific to the dMRI methodology and parameters used.

95 Applying the conversion factor to the inter-parcel connectivity from our prior study yields an
96 estimate of the absolute number of axons connecting different cortical areas (*Figure 1A*), 1.05×10^9
97 axons in total. Axons are approximately log-normally distributed among non-adjacent parcel pairs,
98 with adjacent pairs having disproportionally high axon counts (*Figure 1B*). The total count of a parcel's
99 axons to or from all other areas is much less variable when normalized by the parcel's area (*Figure 1*

100 *D*,*E*). Multiplying the total number of fibers by the effective fiber cross-sectional area (the inverse
101 callosal packing density, 6.2×10^{-6} mm^2/axon) yields 6.6×10^3 mm^2 of cortex or 3.7% of the total white-
102 gray interface. Note that the effective axonal area includes myelin, supporting cells and intercellular
103 space in addition to the axon proper. The percent of fiber-allocated cortical area is quite similar to the
104 ~4% of total cortical fibers Shülz and Braitenburg estimated [8] are contained in the corpus callosum
105 and long fascicles. The remaining ~95% of the cortical gray-white interface area is likely occupied by
106 the short range U-fiber system which is difficult to assess with dMRI.

107 The volume of hemispheric white matter (WM) occupied by axons between cortical parcels is equal
108 to the sum of all axons' lengths multiplied by their cross-sectional areas. The mean fiber tract lengths of
109 connections were taken from our prior dMRI analysis [3]. For the effective cross-sectional area of axons
110 we again used the inverse of the callosal fiber density [5]. So calculated, the volume occupied by
111 cortico-cortical and hippocampo-cortical fibers is 4.3×10^5 mm^3, or about 96% of the total MRI-assessed
112 WM volume. This implies that the number of long-range fibers cannot be larger than our estimate
113 unless the callosal fiber density measurement is mistakenly low. The remaining WM volume may seem
114 insufficient for connections with subcortical structures. However, the major subcortical structures
115 known to communicate with the cortex (thalamus, amygdala, striatum, nucleus basalis, locus coeruleus,
116 etc.) contain, in sum, less than 1% of the number of cortical neurons [9,10]. Even under the unlikely
117 assumption that all excitatory thalamic neurons project to all cortical parcels proportionally to their
118 area, their axons would only comprise ~4% of the total WM volume.

119 Discussion

120 Our estimation of the absolute number of axons interconnecting cortical areas depends on
121 assumptions of callosal axon packing density, proportionally between the number of axons connecting
122 two areas and dMRI tractography for the areal pair, and approximate parity between dMRI sensitivity to

inter- and intra-hemispheric connections. Although there are only two reports of axonal density in the corpus callosum, they are consistent with each other and with reports of axonal density of intrahemispheric tracts. Our study relies on the data reported by Aboitiz et al. [11], because it is the most systematic count of which we are aware. There is one later study, Liewald et al. [12], which provides a value only slightly lower, 1.23×10^5 vs 1.6×10^5 axons/mm^2 after correction for tissue shrinkage. And because this study was primarily a survey of axon diameter with packing density only incidentally recorded, it is conceivable that density values derived from could be small underestimates. Mis-estimated tissue shrinkage is possible but likely to be <10% and callosal areas were measured with a well-validated and widely-used method [4]. Concerning dMRI- to-axon-count proportionality, it has been shown in macaques that there is a strong linear correlation between dMRI-traced streamlines and the number of fibers identified with retrograde tracers connecting regions the cortex [6]. We found a similar, though understandably weaker, correlation among homologous connections between human dMRI and macaque histology in our prior study [3].

Furthermore, we found little difference between distance-matched dMRI connectivity for callosal versus ipsilateral connections (*Figure 1C*). If callosal axons were more easily detectable, this would be reflected as an upward displacement of the blue trace above the green trace across the entire distance domain, which is not evident. This parity is perhaps unsurprising because over most of their trajectories, inter-hemispheric fibers are subjected to the same crossing fiber issues as intra-hemispheric. Specifically, the corpus callosum is a distinct tract for only about 15-35 mm, but its fibers range in length up to about 300 mm. Of course, short interhemispheric trajectories are dominated by the callosal segment, and long by the intrahemispheric segments. Generally, the proportion of their trajectories that are within the callosum is roughly proportional to their length. Consequently, if there were enhanced detection of callosal fibers as streamlines by dMRI, the green trace in figure 1C would

146 be expected to be elevated primarily at short fiber lengths, resulting in a noticeably steeper slope for
147 the blue than the green trace, which again is not observed. These data support the applicability of the
148 scaling factor derived from interhemispheric fibers to intrahemispheric fibers.

149 While we derive a single dMRI-to-axon count factor, it is possible that the true conversion ratio
150 varies somewhat among connections due to local microstructural differences other than axon count
151 such as axon caliber, packing density, or myelination. However, the major fasciculi (including the
152 corpus callosum) have similar axon calibers and packing densities [12], as expected given that
153 different sections of the same long-range fibers contribute to the composition of several fasciculi. More
154 generally, packing density is a function of local cellular interactions, especially oligodendrocytes, and
155 because these are the same in the corpus callosum and intrahemispheric white matter, the *a priori*
156 expectation is that packing density would be similar, as histological data supports. Myelination has
157 only a modulatory effect on dMRI-detected anisotropy, with most of the effect derived from axonal
158 membranes [13]. Nevertheless, microstructural variation in dMRI-to-axon count ratio is a possible
159 source of noise in our estimate. We evaluated the effects the potential mis-specification of these critical
160 parameters on our estimates of axonal connections and found that they would result in only modest
161 changes of axonal connectivity. For example, using the alternative value for callosal axon packing
162 density (1.23×10^5 [14] rather than 1.60×10^5 axons/mm^2 [11]) decreases the estimated number of
163 axons between Wernicke's and Broca's areas from 25,310 to 19,310; assuming a 75% [15] rather than
164 65% linear shrinkage coefficient [11] increases the estimated number of axons from 25,310 to 33,690.
165 Thus, our basic conclusions seem to be robust within plausible ranges of these parameters.

166 The simple scaling factor we derive here permits some interesting quantitative estimates which may
167 inform models of cortical neurophysiology. For example, the connections between Wernicke's and
168 Broca's areas are thought to integrate receptive and expressive aspects of language, but there are only

169 ~25,000 axons between the core cortical parcels in these regions (parcels 44 and PSL), fewer than the
170 number of words in a college student's vocabulary [16]. Areas distant from the hippocampus, notably
171 the dorsolateral prefrontal cortex, may be connected to it by <10 axons/mm^2 (*Figure 1F*). On a global
172 scale, we estimate the total number of inter-areal axons as 1.05×10^9, implying that <5% of the
173 ~11.5×10^9 cortical pyramidal cells [17] project outside their area (because only half of the axons are
174 efferent). Furthermore, since 51% of those are to adjacent areas, <2.5% of pyramidal cells project
175 beyond the adjacent parcel. This sparse long-range connectivity is consistent with its exponential fall-
176 off measured with dMRI in humans and histologically in other mammals [3,18].
177 These constraints encourage consideration of models of cortical function where connections are
178 dense but mainly local. Neural models with multiple paths between cortical neurons due to numerous
179 short connections can show long-range covariance and even synchrony [19,20], and these have been
180 observed experimentally in humans [21]. In such models, cortical locations interact through activation
181 of multi-synaptic pathways rather than direct connections, and the key to connectivity is physiological
182 selection under multiple constraints rather than anatomical projections. Lastly, it is useful to note that
183 these quantitative considerations are radically different in other species, where the smaller number of
184 cortical neurons and shorter inter-areal distances allow greater connectivity between cortical areas, as
185 well as a larger proportion of subcortical connectivity.
186

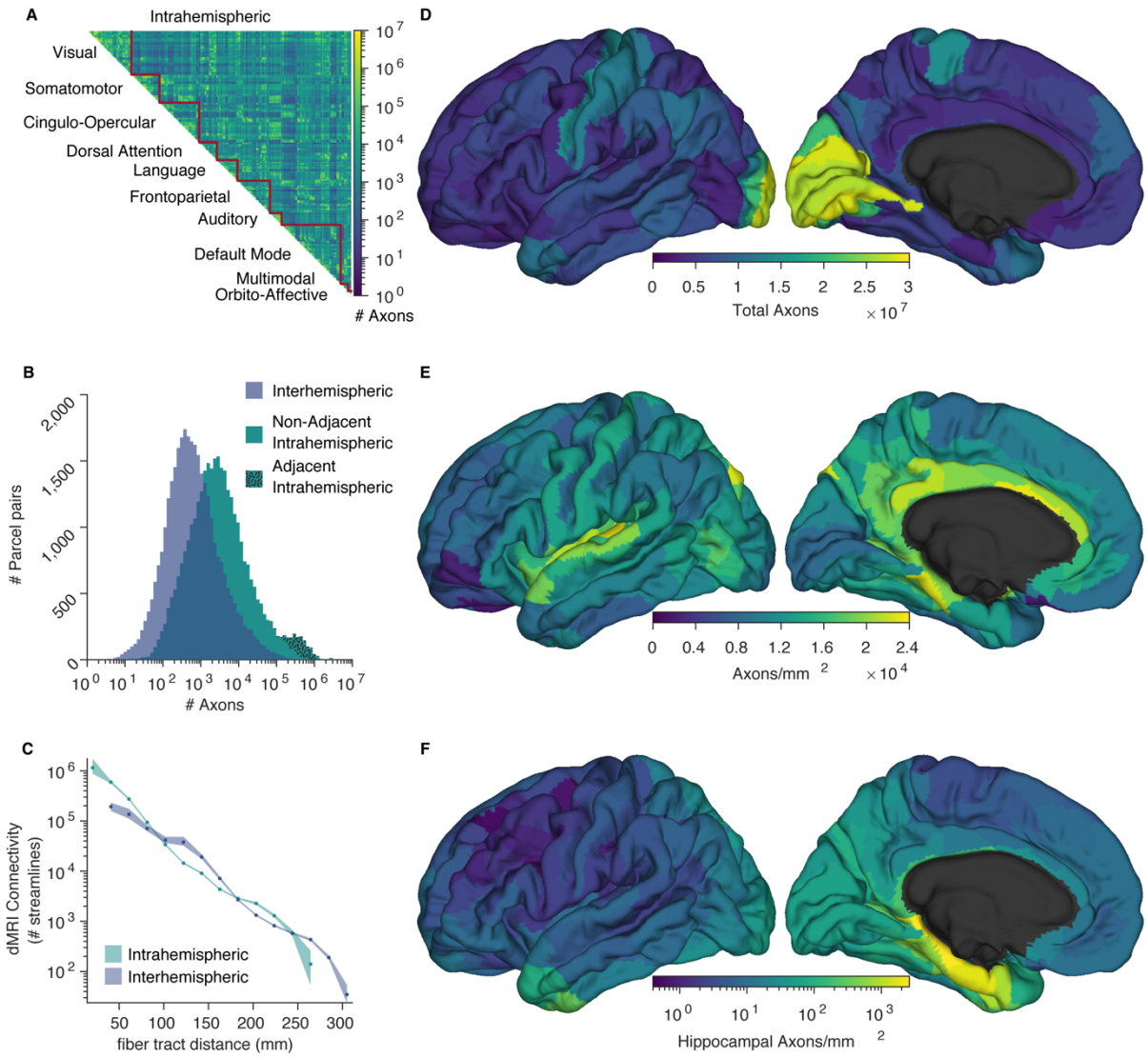

Figure 1. The number of axons connecting interconnecting the 360 cortical parcels of the HCP-MMP1.0 atlas. (A) Connectivity matrix of intrahemispheric axon counts, averaged across the two hemispheres. Parcels are ordered into 10 functional networks. (B) Histograms showing the distribution of inter- and intrahemispheric pairwise axon counts. Physically adjacent and non-adjacent parcel pair intrahemispheric histograms are stacked. Median connectivity is ~2,700 axons between cortical areas in the same hemisphere, and 540 interhemispherically. (C) dMRI connectivity as a function fiber tract distance. Pairwise values averaged within 15 fiber-length bins. Shading shows bootstrapped 95% confidence intervals. (D-F) axons counts and densities averaged across the two hemispheres and

visualized on the left fsaverage template cortex. (D) total axons connecting each parcel to all others. (E) axons connecting each parcel to all others, normalized by the reference parcel's area. (F) axons connecting the hippocampus to the rest of the cortex, normalized by the area of the cortical parcel, shown in log scale.

Acknowledgements

This work was supported by National Institutes of Health grants RF1MH117155 and R01NS109553 (EH). Data were provided, in part, by the Human Connectome Project, WU-Minn Consortium (Principal Investigators: David Van Essen and Kamil Ugurbil; 1U54MH091657) funded by the 16 National Institutes of Health (NIH) Institutes and Centers that support the NIH Blueprint for Neuroscience Research; and by the McDonnell Center for Systems Neuroscience at Washington University.

Data availability

The processed data used in this study are available at https://doi.org/10.5281/zenodo.4910310. Datafiles are in Matlab v7.3 format. The Human Connectome Project's raw imaging data and FreeSurfer outputs may be downloaded from https://db.humanconnectome.org.

Code availability

The main standalone analysis Matlab code used in this study is available at https://doi.org/10.5281/zenodo.4910310. Additional non-standalone supporting code will be made available upon request.

References

1. Geschwind N. Disconnexion syndromes in animals and man. Brain. 1965;88: 237–294.
2. Assaf Y, Johansen-Berg H, Thiebaut de Schotten M. The role of diffusion MRI in neuroscience. NMR Biomed. 2019;32: e3762. doi:https://doi.org/10.1002/nbm.3762
3. Rosen BQ, Halgren E. A Whole-Cortex Probabilistic Diffusion Tractography Connectome. eNeuro. 2021;8: ENEURO.0416-20.2020. doi:10.1523/ENEURO.0416-20.2020
4. Fischl B. FreeSurfer. Neuroimage. 2012;62: 774–781. doi:10.1016/j.neuroimage.2012.01.021
5. Aboitiz F, Scheibel AB, Fisher RS, Zaidel E. Fiber composition of the human corpus callosum. Brain Res. 1992;598: 143–153. doi:10.1016/0006-8993(92)90178-C
6. Donahue CJ, Sotiropoulos SN, Jbabdi S, Hernandez-Fernandez M, Behrens TE, Dyrby TB, et al. Using Diffusion Tractography to Predict Cortical Connection Strength and Distance: A Quantitative Comparison with Tracers in the Monkey. J Neurosci. 2016;36: 6758–6770. doi:10.1523/JNEUROSCI.0493-16.2016
7. Glasser MF, Coalson TS, Robinson EC, Hacker CD, Harwell J, Yacoub E, et al. A multi-modal parcellation of human cerebral cortex. Nature. 2016;536: 171–8. doi:10.1038/nature18933
8. Schüz A, Braitenberg V. The human cortical white matter: quantitative aspects of cortico-cortical long-range connectivity. Cortical areas Unity Divers. 2002; 377–385.
9. Arcelli P, Frassoni C, Regondi MC, De Biasi S, Spreafico R. GABAergic neurons in mammalian thalamus: a marker of thalamic complexity? Brain Res Bull. 1997;42: 27–37.
10. Avino TA, Barger N, Vargas M V, Carlson EL, Amaral DG, Bauman MD, et al. Neuron numbers increase in the human amygdala from birth to adulthood, but not in autism. Proc Natl Acad Sci. 2018;115: 3710–3715.
11. Aboitiz F, Scheibel AB, Fisher RS, Zaidel E. Fiber composition of the human corpus callosum. Brain Res. 1992;598: 143–153.
12. Liewald D, Miller R, Logothetis N, Wagner HJ, Schüz A. Distribution of axon diameters in cortical white matter: an electron-microscopic study on three human brains and a macaque. Biol Cybern. 2014;108: 541–557. doi:10.1007/s00422-014-0626-2
13. Beaulieu C. The basis of anisotropic water diffusion in the nervous system – a technical review. NMR Biomed. 2002;15: 435–455. doi:https://doi.org/10.1002/nbm.782
14. Liewald D, Miller R, Logothetis N, Wagner H-J, Schüz A. Distribution of axon diameters in cortical white matter: an electron-microscopic study on three human brains and a macaque. Biol Cybern. 2014;108: 541–557.
15. Kretschmann HJ, Tafesse U, Herrmann A. Different volume changes of cerebral cortex and white matter during histological preparation. Microsc Acta. 1982;86: 13–24.
16. Brysbaert M, Stevens M, Mandera P, Keuleers E. How Many Words Do We Know? Practical Estimates of Vocabulary Size Dependent on Word Definition, the Degree of Language Input and the Participant's Age . Frontiers in Psychology . 2016. p. 1116. Available: https://www.frontiersin.org/article/10.3389/fpsyg.2016.01116
17. Azevedo FAC, Carvalho LRB, Grinberg LT, Farfel JM, Ferretti REL, Leite REP, et al. Equal numbers of neuronal and nonneuronal cells make the human brain an isometrically scaled-up primate brain. J Comp Neurol. 2009;513: 532–541. doi:10.1002/cne.21974
18. Wang X-J. Neurophysiological and computational principles of cortical rhythms in cognition. Physiol Rev. 2010;90: 1195–268. doi:10.1152/physrev.00035.2008
19. Bazhenov M, Rulkov NF, Timofeev I. Effect of synaptic connectivity on long-range synchronization of fast cortical oscillations. J Neurophysiol. 2008;100: 1562–1575. doi:10.1152/jn.90613.2008
20. Vicente R, Gollo LL, Mirasso CR, Fischer I, Pipa G. Dynamical relaying can yield zero time lag neuronal synchrony despite long conduction delays. Proc Natl Acad Sci. 2008;105: 17157 LP – 17162. doi:10.1073/pnas.0809353105
21. Dickey CW, Verzhbinsky IA, Jiang X, Rosen BQ, Kajfez S, Stedelin B, et al. Widespread ripples synchronize human cortical activity during sleep, waking, and memory recall. bioRxiv. 2021; 2021.02.23.432582. doi:10.1101/2021.02.23.432582

S1 Appendix: Extended Methods

Diffusion MRI

The dMRI connectivity data used to estimate inter-parcel axon totals was described in our prior report [1] whose data are available in full at https://doi.org/10.5281/zenodo.4060485. Preprocessed imaging data for 1,065 healthy young adults were retrieved from the Human Connectome Project WU-Minn consortium 1200 release [2] (https://db.humanconnectome.org). We segmented the cortex into 180 parcels per hemisphere following the HCP-MMP1.0 atlas[3] and performed probabilistic tractography using the probtrackX tool [4] from FSL [5] using tractography parameters detailed in our prior report [1]. This analysis yielded a 360 x 360 dMRI connectivity matrix for each subject which provided the example data for applying the method presented here. For probtrackX-derived connectivity, the raw unit of dMRI connectivity strength is the number of streamlines connecting seed and target regions. The absolute magnitude of this metric is arbitrary as it scales with the number of samples drawn from the probability distribution of diffusion parameters in each voxel, in our analysis 5,000. Note that the method described here is largely agnostic to the dMRI methodology, provided it returns a continuous connectivity metric and has relatively equal sensitivity to callosal and ipsilateral connections.

Cross-sectional area of the corpus callosum, white matter volume, and parcel areas

The HCP WU-Minn consortium 1200 release [2] includes the standard outputs from the FreeSurfer `recon-all` pipline [6]. With default parameters, this pipeline labels the 1 mm^3 voxels of the `aseg.mgz` volume which contain the corpus callosum with a fixed 5mm lateral extent. Dividing the number of callosum-label voxels by 5 yields an estimate of its cross-sectional area, in mm^2. The total white matter volume is reported in the `aseg.stats` output of `mri_segstats`. Parcel areas and adjacency were

301 determined [7] on triangular mesh of each subject's reconstruct white matter surface, or white matter –
302 gray matter interface (`?h.white`).
303

304 ## Estimate of callosal fiber density

305 Our estimate of callosal fiber density was based on the electron microscopy (EM) study of Aboitiz
306 and colleagues [8] who reported a fiber density of 38 per 100 μm^2 or 1.6×10^5 axons/mm^2 after
307 accounting for 65% linear tissue shrinkage after fixation. This is concordant with their finding of
308 1.57×10^5 axons/mm^2 as measured with light-microscopy in twenty brains as well as the 1.23×10^5 non-
309 exhaustively counted axons per mm^2 reported in a more recent EM study [9] of callosal axon diameter
310 in two brains [9], assuming the same degree of tissue shrinkage.
311

312 ## Distance matched Intra- vs. Interhemispheric dMRI connectivity

313 One assumption of the method described in this report is that the dMRI tractography methodology
314 has approximately similar sensitivity to callosal and ipsilateral connections. This is difficult to determine
315 without ground truth connectivity, as intra- and interhemispheric connections may have true
316 anatomical differences. Nevertheless, we examined distance-matched intra- vs interhemispheric
317 connections (Figure 1*C*) and found no statistical evidence that they are different. Pairwise connections
318 were averaged in 15 distance bins, log-transformed and linear fits obtained for intra- and
319 interhemispheric connections. For the overlapping distance domain, the intrahemispheric slope is -
320 0.30, 95% confidence interval = [-0.33 -0.26] with an intercept of 6.18 [5.91 6.45] and the
321 interhemispheric slope is -0.26 [-0.29 -0.24] and intercept of 5.93 [5.72 6.14]; the 95% confidence
322 intervals of both parameter are overlapping. In addition, a paired r-test of correlation differences [10]
323 failed to reject the null hypothesis, $p = 0.58$. The parity between distance-matched intra- and

interhemispheric connections also holds when the linear fit is obtained for over the entire distance domain, with an intrahemispheric slope and intercept -.31 [-0.33 -0.28] and 6.24 [6.01 6.46], respectively; -.28 [-0.30 -0.25] and 6.00 [5.78 6.23] for interhemispheric connections.

Estimating axon counts and axon volume from dMRI

From the histological estimate of callosal fiber density, MRI-derived measures of callosal cross-sectional area and white matter connectivity, the conversion factor between dMRI connectivity and physical axons can be estimated as follows:

Eq. 1.1 $N_{callosum} = A_{callosum} * D_{callosum}$

Eq. 1.2 $C_{axon} = \frac{Ncallosum}{M_{dMRI}}$

Where $A_{callosum}$ is the cross-sectional area (mm^2), $D_{callosum}$ is the assumed fiber density ($1.6x10^5$ axons/mm^2) of the corpus callosum, $N_{callosum}$ is the estimated total number of callosal fibers, M_{dMRI} is the magnitude of dMRI callosal connectivity, in our case, the number of tractography streamlines, and C_{axon} is the conversion factor from dMRI to physical fibers (axons/streamline).

In addition to connectivity strength, or number of streamlines, the dMRI tractography analysis also yields a mean streamline length for every parcel-pair connection. After converting dMRI connectivity strength to physical axon count as described above, the total volume of the estimated axons can be calculated as follows:

Eq. 2.1 $WM_{volume} = \sum_{i=1}^{N_{pair}} l_i * n_i * C_{axon} * \frac{1}{D_{callosum}}$

Eq. 2.2 $WM_{volume} = \sum_{i=1}^{N_{pair}} l_i * n_i * \frac{A_{callosum}}{M_{dMRI}}$

Where WM_{volume} is the estimated axonal white matter volume (mm^3) and N_{pair} is the total number of parcel pairs. l_i and n_i are the length (mm) and number of dMRI streamlines in the ith parcel pair. Eq. 2.1 can be simplified into Eq. 2.2 by substituting Eqs. 1.1 and 1.2 into 2.1.

Parcel ordering

The parcel ordering and the ten functional networks shown in Fig 1*A* were defined in our previous report [1] and were modified from twelve networks identified by Ji and colleagues in a resting-state fMRI study on the HCP cohort [11].

Thalamocortical fiber volume estimation

The scope of our previous dMRI tractography study [1] was confined to corticocortical (including cortico-hippocampal) connectivity. In order to estimate the total volume of thalamocortical axons, we assumed a total axon count of 22.6×10^6 as reported by histological count [12] and allocated these axons to cortical parcels in proportion to their area. The inverse callosal packing density was used for effective cross-sectional area, as with corticocortical connections. To estimate the length of thalamocortical fiber tracts, for each parcel i, we first identified the thalamic voxel nearest to parcel's centroid. We then used the interparcel fiber tract length [1] from the centroid of parcel i to the identified parathalamic parcel centroid. To this figure we added the Euclidean distance from the parathalamic centroid to the nearest voxel of the thalamus, ensuring that estimated thalamocortical fiber tract length is always non-zero. As with corticocortical connections, the total white matter volume of each connection was estimated by taking the product of the number of axons, the effective cross-sectional area, and the estimated fiber tract length (Eq. 2).

References

1. Rosen BQ, Halgren E. A Whole-Cortex Probabilistic Diffusion Tractography Connectome. eNeuro. 2021;8: ENEURO.0416-20.2020. doi:10.1523/ENEURO.0416-20.2020
2. Van Essen DC, Smith SM, Barch DM, Behrens TEJ, Yacoub E, Ugurbil K. The WU-Minn Human Connectome Project: An overview. Neuroimage. 2013;80: 62–79. doi:10.1016/j.neuroimage.2013.05.041
3. Glasser MF, Coalson TS, Robinson EC, Hacker CD, Harwell J, Yacoub E, et al. A multi-modal parcellation of human cerebral cortex. Nature. 2016;536: 171–8. doi:10.1038/nature18933
4. Behrens TEJ, Berg HJ, Jbabdi S, Rushworth MFS, Woolrich MW. Probabilistic diffusion tractography with multiple fibre orientations: What can we gain? Neuroimage. 2007;34: 144–155. doi:10.1016/j.neuroimage.2006.09.018
5. Jenkinson M, Beckmann CF, Behrens TEJ, Woolrich MW, Smith SM. FSL. Neuroimage. 2012;62: 782–790. doi:10.1016/j.neuroimage.2011.09.015
6. Fischl B. FreeSurfer. Neuroimage. 2012;62: 774–781. doi:10.1016/j.neuroimage.2012.01.021
7. Meyer M, Desbrun M, Schröder P, Barr AH. Discrete Differential-Geometry Operators for Triangulated 2-Manifolds. 2003. pp. 35–57. doi:10.1007/978-3-662-05105-4_2
8. Aboitiz F, Scheibel AB, Fisher RS, Zaidel E. Fiber composition of the human corpus callosum. Brain Res. 1992;598: 143–153. doi:10.1016/0006-8993(92)90178-C
9. Liewald D, Miller R, Logothetis N, Wagner HJ, Schüz A. Distribution of axon diameters in cortical white matter: an electron-microscopic study on three human brains and a macaque. Biol Cybern. 2014;108: 541–557. doi:10.1007/s00422-014-0626-2
10. Williams EJ. The comparison of regression variables. J R Stat Soc Ser B. 1959;21: 396–399.
11. Ji JL, Spronk M, Kulkarni K, Repovš G, Anticevic A, Cole MW. Mapping the human brain's cortical-subcortical functional network organization. Neuroimage. 2019;185: 35–57. doi:10.1016/j.neuroimage.2018.10.006
12. Arcelli P, Frassoni C, Regondi MC, De Biasi S, Spreafico R. GABAergic neurons in mammalian thalamus: a marker of thalamic complexity? Brain Res Bull. 1997;42: 27–37.